Available online at www.sciencedirect.com
SCIENCE DIRECT
Biochemical and Biophysical Research Communications 337 (2005) 1237–1248
BBRC
www.elsevier.com/locate/ybbrc

Glyoxalase I from *Leishmania donovani*: A potential target for anti-parasite drug

Prasad K. Padmanabhan [a], Angana Mukherjee [a], Sushma Singh [a], Swati Chattopadhyaya [a], Venkataraman S. Gowri [b], Peter J. Myler [c], Narayanaswamy Srinivasan [b], Rentala Madhubala [a,*]

[a] *School of Life Sciences, Jawaharlal Nehru University, New Delhi 110067, India*
[b] *Molecular Biophysics Unit, Indian Institute of Science, Bangalore, India*
[c] *Seattle Biomedical Research Institute, 4 Nickerson Street, Seattle, WA 98109-1651, USA*

Received 26 September 2005
Available online 7 October 2005

Abstract

Glyoxalases are involved in a ubiquitous detoxification pathway. In pursuit of a better understanding of the biological function of the enzyme, the recombinant glyoxalase I (LdGLOI) protein has been characterized from *Leishmania donovani*, the most important pathogenic *Leishmania* species that is responsible for visceral leishmaniasis. A 24 kDa protein was heterologously expressed in *Escherichia coli*. LdGLOI showed a marked substrate specificity for trypanothione hemithioacetal over glutathione hemithioacetal. Antiserum against recombinant LdGLOI protein could detect a band of anticipated size ~16 kDa in promastigote extracts. Several inhibitors of human GLOI showed that they are weak inhibitors of *L. donovani* growth. Overexpression of GLOI gene in *L. donovani* using *Leishmania* expression vector pspα hygroα, we detected elevated expression of GLOI RNA and protein. Comparative modelling of the 3-D structure of LDGLOI shows that substrate-binding region of the model involves important differences compared to the homologues, such as *E. coli*, specific to glutathione. Most notably a substrate-binding loop of LDGLOI is characterized by a deletion of five residues compared to the *E. coli* homologue. Further, a critical Arg in the *E. coli* variant at the substrate-binding site is replaced by Tyr in LDGLOI. These major differences result in entirely different shapes of the substrate-binding loop and presence of very different chemical groups in the substrate-binding site of LDGLOI compared to *E. coli* homologue suggesting an explanation for the difference in the substrate specificity. Difference in the substrate specificity of the human and LDGLOI enzyme could be exploited for structure-based drug designing of selective inhibitors against the parasite.

Keywords: *Leishmania donovani*; Recombinant glyoxalase I; Overexpression; Inhibitors; Structural analysis

Leishmania donovani, a flagellated protozoan parasite, is the causative agent of visceral leishmaniasis. Sandflies transmit promastigote forms of the parasite to the mammalian host, where they invade macrophages and transform into amastigotes. Pentavalent antimonials are the standard first-line treatment for leishmaniasis [1,2], although resistance is a growing problem [3]. The aromatic diamidine pentamidine represents a second line of treatment [4]. Current chemotherapeutic agents are unsuitable, in part because of their high toxicity and the emergence of drug resistance. Thus, identification of novel chemotherapeutic targets is of tremendous economic and medical importance. Leishmanial patient's refractoriness to existing drugs and the availability of a limited repertoire of drugs have become rapidly growing problems. Hence there is an urgent need for the development of new drugs against leishmaniasis.

The glyoxalase system is a ubiquitous detoxification pathway that protects against cellular damage caused by methylglyoxal, a mutagenic and cytotoxic compound that is mainly formed as a by-product of glycolysis. It is also formed during catabolism of amino acids via aminoacetone

* Corresponding author. Fax: +91 11 26106630.
E-mail address: madhubala@mail.jnu.ac.in (R. Madhubala).

0006-291X/$ - see front matter © 2005 Elsevier Inc. All rights reserved.
doi:10.1016/j.bbrc.2005.09.179

and hydroxyacetone [5]. The glyoxalase system comprises of two enzymes, glyoxalase I (GLOI) (lactoylglutathione lyase, EC 4.4.1.5) and glyoxalase II (GLOII) (hydroxyacylglutathione hydrolase, EC 3.1.2.6). Glyoxalase I catalyses the formation of *S*-D-lactoyl glutathione from the hemithioacetal formed nonenzymatically from methylglyoxal and glutathione. Glyoxalase II converts *S*-D-lactoyl glutathione to lactate and free glutathione [6]. Thus, glutathione acts as a cofactor in the overall reaction pathway. The glyoxalase system is present in the cytosol of cells and cellular organelles particularly mitochondria. It is found throughout biological life and is thought to be ubiquitous [7]. The widespread distribution suggests it fulfills a function of fundamental importance to biological life. Glyoxalase has a distinct role in cell proliferation and maturation [8]. Glyoxalase enzyme activities have been reported as the earliest phenotypes expressed in embryogenesis [8]. In tumor tissues, high activities of glyoxalase I has also been reported [9]. The main source of energy for uncontrolled cell division and proliferation in tumor tissues is glycolysis that produces methylglyoxal, which in turn is detoxified by glyoxalase system. However, despite its ubiquitous distribution little is known about its function. Inhibitors of glyoxalase I have been reported to be selectively toxic to proliferating cells, which could be due to increased accumulation of methylglyoxal that could lead to inhibition of DNA synthesis [10,11]. Glyoxalase I inhibitors have also been reported to have antimalarial [12] and antitrypanosomal activities [13]. The glyoxalase I activity has been reported in *Leishmania braziliensis* [14] but very low levels of GLOI and GLOII activities were detected in lysates using glutathione as the substrate [15]. Glyoxalase system of the pathogenic kinetoplastids has been recently reported to be unique, as a consequence of these protozoa possessing an unusual thiol metabolism. In these organisms, instead of glutathione, the major low molecular mass thiol is trypanothione [N^1,N^8-bis(glutathionyl)spermidine] [16]. It has been recently reported that the GLOI system in *Leishmania major* uses trypanothione as the substitute for glutathione [16]. The metal cofactor is zinc in eukaryotes and nickel in *Escherichia coli* [17,18] and *L. major* [16]. Thus, both the substrate and cofactor of leishmanaia glyoxalase are different from those of mammalian glyoxalases. The difference in cofactor dependence is reflected in differences between the active sites of the human and *Leishmania* enzymes, suggesting that the latter may be a target for antimicrobial therapy [19,20].

While biological phenomena characterized in one *Leishmania* species are frequently taken as pointers to similar activity in other species of the genus, it is important to actually study each individual species. Crucial differences between species exist, and this is clearly manifest in pharmacological responses to drug. In this paper, we describe the characterization of glyoxalase I from *L. donovani*, the most important pathogenic *Leishmania* species that is responsible for visceral leishmaniasis in India. Using the comparative modelling approach we also examined the plausible structure of LdGLOI based on the available crystal structure of human, yeast, and *E. coli* GLOI. The 3-D model generated on the basis of the close homologue from *E. coli* enabled identification of major changes in the shape and residues in the putative active site of LdGLOI compared to *E. coli* variant thus providing a possible explanation for the different substrate specificity.

Materials and methods

Parasite and culture condition. Leishmania donovani AG83 (MHOM/IN/1983/AG83) promastigotes and strain 2001, a field isolate of *L. donovani*, were cultured at 22 °C in modified M199 medium (Sigma, USA) supplemented with 100 U/ml penicillin (Sigma, USA), 100 μg/ml streptomycin (Sigma, USA), and 10% heat-inactivated fetal bovine serum (FBS) (Gibco/BRL, Life Technologies Scotland, UK).

Axenic amastigotes were obtained after transformation of promastigotes to amastigotes and were grown in RPMI-1640 medium (pH 5.5) supplemented with 100 U/ml penicillin, 100 μg/ml streptomycin sulfate and 20% heat-inactivated serum in a CO_2 incubator (5% CO_2) at 37 °C. Axenically grown amastigote forms of the cloned wild type strains of *L. donovani* were maintained by weekly passages in RPMI 1640 (pH 5.5) supplemented with 100 U/ml penicillin, 100 μg/ml streptomycin, and 20% heat inactivated serum in a CO_2 incubator (5% CO_2) at 37 °C. From a starting inoculum of 5×10^5 amastigotes/ml, cell densities in the range of 2×10^7–5×10^7 parasites/ml were obtained on day 7. The population of axenically grown amastigotes appeared homogeneous, round to ovoid, aflagellate, and immobile [21].

Nucleic acid isolation, pulse field gradient gel electrophoresis (PFGE), and hybridization analysis. Genomic DNA was isolated from $\sim 2 \times 10^9$ *L. donovani* AG83 promastigotes by standard procedures [22], digested with different restriction endonucleases, and subjected to electrophoresis in 0.8% agarose gels. The fragments were transferred to nylon membrane (Amersham Pharmacia Biotech) and subjected to Southern blot analysis.

Total RNA was isolated from 2×10^8 *L. donovani* wild type promastigotes and from GLOI overexpressing strain using TRI reagent (Sigma). For Northern blot analysis, 15 μg of total RNA was fractionated by denaturing agarose gel electrophoresis and transferred onto nylon membrane following standard procedures.

Leishmania chromosomes were separated by PFGE in which low melting agarose blocks, containing embedded cells (10^8 log phase promastigotes/ml), were electrophoresed in a contour clamped homogenous electric field apparatus (CHEF DRIII, Bio-Rad) in 0.5× TBE, with buffer circulation at a constant temperature of 14 °C. *Saccharomyces cerevisiae* chromosomes were used as size markers. Pulse field gel electrophoresis (PFGE) running conditions were as follows: initial switch time, 60 s; final switch time, 120 s; run time, 24 h; current 6 V/cm; including angle 120°. Following the transfer of DNA, RNA, and chromosomes onto nylon membranes, the membranes were rinsed in 2× SSC. The nucleic acids were UV cross-linked to the membrane in a Stratagene UV cross-linker. Prehybridization was done at 65 °C for 4 h in a buffer containing 0.5 M sodium phosphate; 7% SDS; 1 mM EDTA, pH 8.0, and 100 μg/ml sheared denatured salmon-sperm DNA. The blots were hybridized with denatured [α-^{32}P]dCTP-labelled DNA probe (PCR probe described for the *L. donovani* GLOI coding region) at 10^6 cpm/ml, which was labelled by random priming (NEB Blot Kit, New England Biolabs). Membranes were washed sequentially as follows: 2× SSC, 0.1% SDS; 1× SSC, 0.1% SDS; 0.5× SSC, 0.1% SDS; 0.2× SSC, 0.1% SDS for 10 min each at 65 °C until the non-specific counts had substantially reduced. Membranes were air-dried and exposed to imaging plate. The image was developed by PhosphorImager (Fuji film FLA-5000, Japan) using Image Quant software.

Cloning of glyoxalase I gene from L. donovani. A 426 bp DNA fragment was amplified from genomic DNA, using a sense primer with a flanking *Bam*HI site, 5′-CGCGGATCCATGCCGTCTCGTCGTATG-3′, that coded for the amino acid sequence MPSRRM at position 1–18, and the antisense primer with a flanking *Hin*dIII site,

5′-CCCAAGCTTTTAGGCAGTGCCCTGCTC-3′, which corresponded to amino acid residues EQGTA including the stop codon, at position 409–426. Polymerase chain reaction (PCR) was performed in a 50 μl reaction volume containing 100 ng of genomic DNA, 25 pmol each of gene-specific forward and reverse primers, 200 μM of each dNTP, 2 mM $MgCl_2$, and 5 U *Taq* DNA polymerase (MBI Fermentas). The condition of PCR was as follows: 94 °C for 10 min, 94 °C for 1 min, 57 °C for 45 s, 72 °C for 45 s, and 35 cycles. Final extension was carried for 10 min at 72 °C. A single 426-bp PCR product was obtained and subcloned in to pGEM-T vector (Promega) and subjected to automated sequencing. Sequence analysis was performed by DNAstar whereas comparison with other sequences of the database were performed using the search algorithm BLAST [23]. Multiple alignment of amino acid sequences was performed using CLUSTALW program. The phylogenetic tree was constructed using PHYLIP style treefile produced by CLUSTALW. The amplified DNA fragment, 426 bp (LdGLO1), was also cloned into the *Bam*HI–*Hin*dIII site of pET-30a vector (Novagen). The recombinant construct was transformed into BL21 (DE3) strain of *E. coli*.

Expression and purification procedure. Expression from the construct pET30a-LdGLOI was induced at OD of 0.6 with 0.5 mM IPTG (Sigma) at 37 °C for different time periods. Bacteria were then harvested by centrifugation and the cell pellet was resuspended in binding buffer (50 mM sodium phosphate buffer, pH 7.5, 10 mM imidazole, pH 7.0, 300 mM sodium chloride, 2 mM phenylmethylsulfonyl fluoride (PMSF), and 30 μl protease inhibitor cocktail). Lysozyme (100 μg/ml) was added to cell suspension and kept on rocking platform for 30 min at 4 °C. The resulting cell suspension was sonicated six times for 20 s with 1 min interval. The lysate was centrifuged at 20,000*g* for 30 min at 4 °C. The resulting supernatant, which contained the protein, was loaded onto a pre-equilibrated Ni–NTA agarose beads (Qiagen). The mixture was kept on a rocking platform for 2 h at 4 °C. It was centrifuged at 400*g* for 30 min at 4 °C. The supernatant was discarded and pellet was washed thrice with wash buffer (50 mM sodium phosphate buffer, pH 7.5; 50 mM imidazole, pH 7.0; 300 mM sodium chloride; 2 mM phenylmethylsulfonyl fluoride (PMSF), and 30 μl protease inhibitor cocktail). The protein was eluted with increasing concentrations of imidazole, pH 7.0. The imidazole was removed by dialysis in 20 mM sodium phosphate buffer, pH 7.5. The purified protein was aliquoted and stored at −80 °C.

Cross-linkage of subunits. The recombinant GLOI protein was cross-linked to 0.1%, 0.05%, and 0.025% glutaraldehyde in phosphate-buffered saline (pH 7.0) [20]. The reaction mixture was incubated for 20 min at 37 °C and analyzed by sodium dodecyl sulfate (SDS)–polyacrylamide gel electrophoresis (SDS–PAGE) using a 10% gel. The protein samples were mixed with an equal volume of loading buffer containing 100 mM Tris–HCl (pH 6.8), 0.4% SDS, 20% glycerol, and 0.001% bromophenol blue, and subjected to boiling in a water bath for 5 min [24].

Preparation of crude lysate of L. donovani for glyoxalase activity. 1×10^8 promastigotes of *L. donovani* were harvested in the late log phase by centrifugation, at 1500*g*, at 4 °C for 15 min, washed with phosphate-buffered saline with 1% glucose (PBSG), pH 7.4. The cell pellet was resuspended in lysis buffer (20 mM Mops, pH 7.2; 1 mM DTT; 2 mM PMSF; 5 μl protease inhibitor cocktail) and incubated on ice for 10 min. The cells were lysed by freeze–thaw in liquid nitrogen. The lysate was centrifuged at 20,000*g* for 30 min at 4 °C and the supernatant was used for GLOI assay as mentioned below.

Protein determination. Protein concentration was determined by the method of Bradford's using bovine serum albumin as standard [25].

Glyoxalase I assay. The activity of recombinant purified glyoxalase I was assayed spectrophotometrically at room temperature by measuring the initial rate of formation of *S*-D-lactoyl trypanothione at 240 nm as described by Racker with slight modification [26]. Trypanothione disulfide (1 mM) (Bachem) was reduced with 3 mM DTT at 60 °C for 20 min before the assay. The resulting reduced trypanothione was used for GLOI assay. The assay mixture contained, in a final volume of 0.5 ml; 100 mM MOPS buffer, pH 7.2; 400 μM methylglyoxal (Sigma); 300 μM reduced trypanothione and 20 μM $NiCl_2$ [16]. The assay mixture was incubated for 10 min followed by the addition of either purified recombinant GLOI protein or crude Leishmania cell lysate. For kinetic studies, the same assay mixture as mentioned above contained either varying concentrations of reduced trypanothione or methylglyoxal with concentrations ranging from 0 to 600 μM each. Trypanothione hemithioacetal concentration was calculated by using the published K_d value of 3 mM for the methylglyoxal–glutathione equilibrium [27]. The value for the $\Delta\varepsilon_{240nm}$ was taken as 2.86 mM^{-1} cm^{-1} for the isomerization of trypanothione hemithioacetal of methylglyoxal [28]. All assays were performed in triplicate.

Antibody production and Western blot analysis. The purified recombinant GLOI protein (20 μg) was subcutaneously injected in mice using Freund's complete adjuvant, followed by two booster doses of recombinant GLOI protein (15 μg) with incomplete adjuvant at two-week intervals to produce the polyclonal antibody against the recombinant GLOI protein. The mice were bled after 2 weeks after the second booster and sera were collected and used for Western blot analysis.

Transfection and overexpression of glyoxalase I gene in Leishmania donovani. The GLO1 ORF was amplified by PCR using a sense primer with a flanking *Xba*I site, 5′-TGCTCTAGAATGCCGTCTCGTCGTATG-3′, that coded for the amino acid sequence MPSRRM at position 1–18, and the antisense primer with a flanking *Hin*dIII site, 5′-CCCAAGCTTTTAGGCAGTGCCCTGCTC-3′, which corresponded to amino acid residues EQGTA including the stop codon, at position 409–426. The amplified DNA fragment (GLO1) was cloned into the *Xba*I–*Hin*dIII site of pspα hygroα *Leishmania* shuttle vector (kindly provided by Dr. Marc Ouellette, Canada) to create pspα hygroα-LdGLO1 containing the hygromycin phosphotransferase gene. Twenty micrograms of the construct was transfected into *L. donovani* promastigotes by electroporation [2 mm gap cuvettes, 450 V, 500 μF (BTX Electro Cell Manipulator 600)]. Transfectants were selected for resistance with hygromycin (40 μg/ml) as described earlier [29].

Sensitivities to cytotoxic drugs. The effects on growth of wild type and GLOI overexpressors by various cytotoxic agents, purpurogallin, flavone, quercetin, and lapachol, were determined in microtiter plates, each containing 96 wells. These compounds were gifts from Dr. Eva Liebau, Hamburg, Germany. Briefly 1×10^6 parasites in 0.2 ml of modified M199 medium with 10% FBS were placed in each well and incubated with various concentrations of the drugs. Two wells in which cells were permitted to grow in the absence of drugs were maintained in parallel as controls. After 72 h of incubation under normal growth condition, cell densities were determined by the Neubauer hemocytometer. The concentrations of the drugs, which inhibited the growth of the wild type and overexpressors by 50%, were determined.

Western blot analysis. Promastigotes and amastigotes were lysed by sonication and cell supernatants were prepared by centrifugation at 20,000*g*. Fifty micrograms of protein from each cell line was fractionated by SDS–polyacrylamide gel electrophoresis blotted onto nitrocellulose membrane using electrophoretic transfer cell (Bio-Rad). Western blot analysis was done using the ECL kit (Amersham Pharmacia Biotech) according to the manufacturer's protocol. Polyclonal antibody to purified recombinant *L. donovani* GLOI generated in mice was used for the Western blot analysis. Autoradiograms were analyzed by using model FLA 5000 imaging densitometer (Fuji, Japan). The results shown are from a single experiment typical of at least three giving identical results.

Comparative modelling of L. donovani glyoxalase I. A model of the 3-D structure of LdGLOI has been generated using the comparative modelling approach. The modelling has been based on the available crystal structure of *E. coli* GLOI [20] which is identified as the closest homologue of LdGLOI of known 3-D structure with good crystallographic resolution of 1.8 Å. The best sequence identity between *E. coli* homologue and LdGLOI is 49%. Another homologue of known structure is from human which has the sequence identity of 33% with LdGLOI. Clearly, modelling LdGLOI on the basis of the crystal structure of homologue from *E. coli* is expected to result in a more accurate model than modelling on the crystal structure of human homologue [30]. The alignment of sequences of several homologues including LdGLOI and homologues from *E. coli* and human is shown in Fig. 1.

Although the 3-D model of LdGLOI has been generated on the basis of crystal structure of *E. coli* variant, the GLOI homologue from human is also used for comparative analysis. This is because several crystal structures

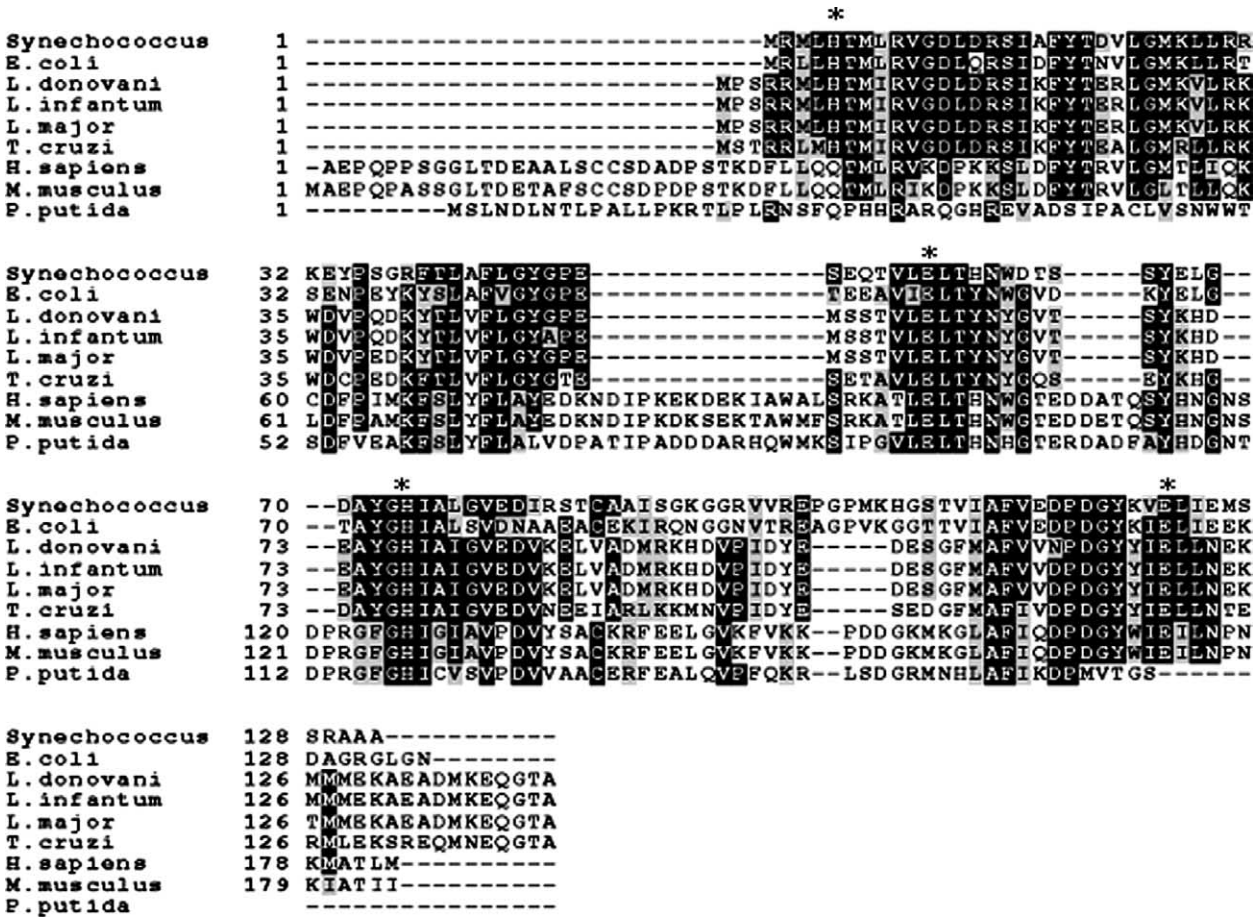

Fig. 1. Multiple sequence alignment of glyoxalase I sequences from *L. donovani* (AAU87880), *L. major* (AY604654), *L. infantum* (LinJ35.2600), *T. cruzi* (Tc00.1047053510743.70), *P. putida* (WZPSLP), *E. coli* (NP_753939), *Synechoccus* sp. WH8102 (NP_898436), *H. sapiens* (Swiss-Prot Accession No. P78375), and *M. musculus* (NP_079650) using CLUSTALW program. The amino acids are numbered to the left of the respective sequences. Residues that are identical or similar with other glyoxalases are indicated in black showing complete identity and gray when they are conserved in at least three sequences. The symbol ∗ indicate amino acids that are responsible for metal binding in the human and *E. coli*.

of human GLOI bound to analogues of the substrate are available and also because both human and *E. coli* homologues show specificity to glutathione while LdGLOI shows specificity to trypanothione.

A 3-D model of LdGLOI has been generated using the suite of programs encoded in COMPOSER [30,31] and incorporated in SYBYL (Tripos, St. Louis). The structurally conserved regions, which are largely α-helical and β-strand regions, in template structures are extrapolated to LdGLOI sequence. The rest of the regions that show high divergence from the sequence of the template structures sequence were modelled by identifying a suitable segment from a dataset of non-identical protein structures. This has been done by a template matching approach, wherein a search is made for the loop segments with required number of residues and that match with the end to end distances of the structurally conserved regions across the three 'anchor' C^{α} on either side of the loop. The hits so obtained are then ranked [32]. The best ranking loop with no short contact with the rest of the structure has been fitted using the ring closure procedure of F. Eisenmenger (unpublished results). Side chains are modelled on the equivalent positions as seen in template structure wherever appropriate or by using rules derived from analysis of known protein structures [33]. The model thus obtained was subject to energy minimization to relieve the short contacts if any.

The model generated using COMPOSER has been subjected to energy minimization using the AMBER force field [34] encoded in the SYBYL software. In the initial rounds of energy minimization, the side chain atoms were allowed to move keeping the backbone position fixed in order to first sort out the short contacts amongst the side chain atoms. In the further rounds, the restriction on the movement of backbone atoms while minimization was also lifted. In the final cycles of minimization, an electrostatic term has been included in the force field. This approach ensured that the LdGLOI model generated is free of short contacts and bad geometry.

Results

Sequence analysis and genomic organization

In order to clone the gene encoding glyoxalase I (GLOI), PCR was performed using specific oligonucleotides, whose sequence was based on *Leishmania* Genome Sequencing Project of *Leishmania infantum* (www.ebi.ac.uk/parasites/LGN/). The sense primer was 5′-CG CGGATCCATGCCGTCTCGTCGTATG-3′, that coded for the amino acid sequence MPSRRM at position 1–18, and the antisense primer with a flanking *Hin*dIII site, 5′-CCCAAGCTTTTAGGCAGTGCCCTGCTC-3′, which corresponded to amino acid residues EQGTA including the stop codon, at position 409–426. Genomic DNA from *L. donovani* AG83 (MHOM/IN/1983/AG83) promastigotes was used as a template. A single 426-bp PCR product

was obtained, cloned, and sequenced. A single open reading frame consisting of 426-bp was isolated (*Leishmania donovani* glyoxalase I gene, GenBank Accession No. AY739896) showing a 96% identity to *L. major* trypanothione-dependent glyoxalase I (GLOI) sequence (GenBank Accession No. AY604654) and 73% identity to *Trypanosoma cruzi*, lactoylglutathione lyase-like protein, putative (Tc00.1047053510743.70).

The open reading frame encoded for putative polypeptide of 141 amino acids, with a predicted molecular mass of 16.3 kDa, which is very similar to *L. major* (141 amino acids), *L. infantum* (141 amino acids), and *T. cruzi* putative lactoylglutathione lyase-like protein (141 amino acids) enzymes but slightly smaller than the human (184 amino acid) and *Psuedomonas putida* (163 amino acid) enzymes (Fig. 1). The predicted isoelectric point (p*I*) of *L. donovani* GLOI was determined to be, pH 4.97, which is comparable to those of proteins from *L. major*, *L. infantum*, and *T. cruzi*. There was only 33% identity between human GLOI (Swiss-Prot Accession No. P78375) and *Leishmania donovani* GLOI (GenBank Accession No. AAU87880) sequences (Fig. 1). The *L. donovani* GLOI protein sequence was found to be 53% identical to *Synechococcus* sp. WH 8102 (GenBank Accession No. NP_898436), 50% identical to *Salmonella typhimurium* (GenBank Accession No. AAC44877), and 49% identical to *E. coli* CFT073 (GenBank Accession No. NP_753939).

A phylogenetic tree has been constructed (Fig. 2) using the *L. donovani* GLOI sequence and other representative GLOI sequences. The tree indicates close evolutionary relationship of *L. donovani* and *T. cruzi* among the kinetoplastid protozoa. The kintoplastid GLOI sequences are closer to *E. coli* and *Synechococcus* sp. enzymes in phylogenetic analysis but have no similarity with human, *M. musculus* and *P. putida*.

To determine the *L. donovani* GLOI gene copy number, Southern blot studies were performed as described under Materials and methods using the 426-bp PCR product as a probe. A single band was obtained (Fig. 3A), revealing that it is a single copy gene. Chromosomal location analysis revealed that *L. donovani* glyoxalase I gene is placed at a single chromosomal band ~2.2 Mb (Fig. 3B). These data concur with the *Leishmania* genome sequencing project findings, according to which glyoxalase I gene has been identified on chromosome 35 (2.2 Mb) in *L. infantum* (www.ebi.ac.uk/parasites/LGN/ chromosome 35.html).

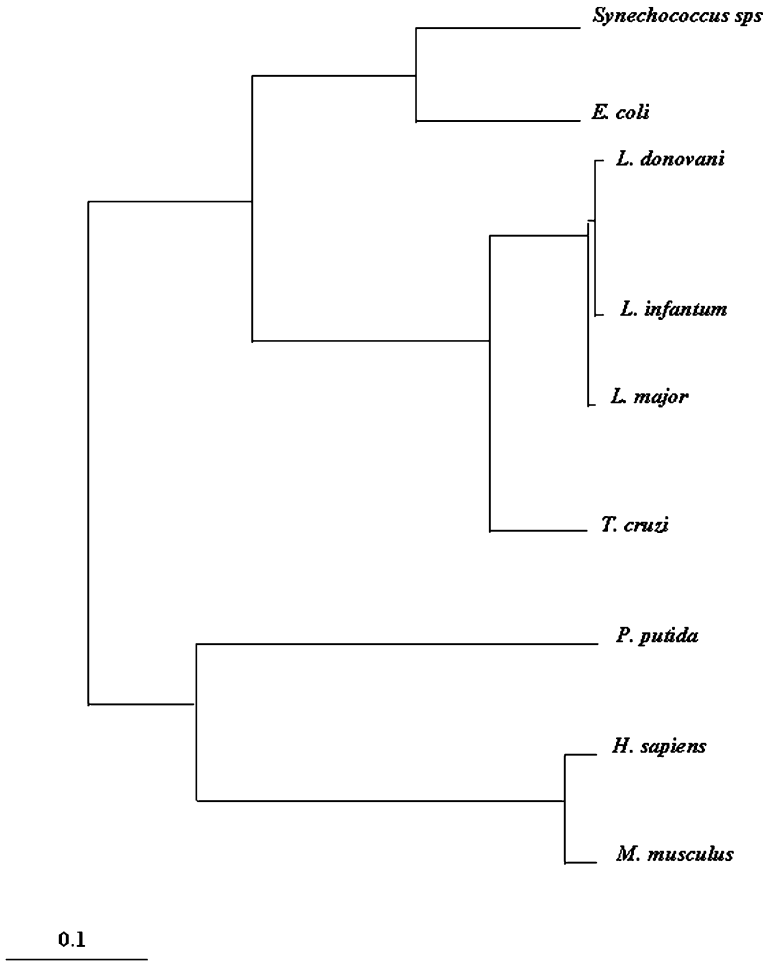

Fig. 2. Phylogenetic tree using the amino acid sequences of glyoxalase I from *L. donovani* and other organisms. The tree view program under the CLUSTALW program viewed the phyletic trees derived from the multiple alignments.

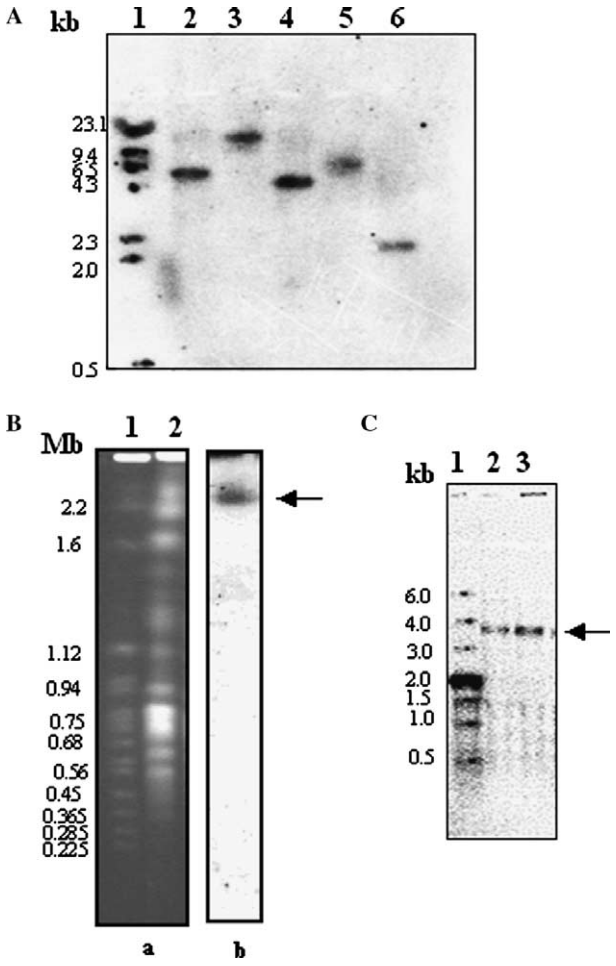

Fig. 3. Genomic organization of glyoxalase I gene in *L. donovani*. (A) Southern blot analysis of *L. donovani* glyoxalase I gene. Lanes 2–6; restriction digests of *L. donovani* genomic DNA with *Eco*RI, *Hin*dIII, *Bam*HI, Sty1, and Sac1, respectively. The blot was probed with 426 bp full-length glyoxalase I gene. Lane 1 represents the DNA molecular weight marker and the sizes are indicated on the left of the figure. (B) PFGE analysis of *L. donovani* indicating chromosomal localization of glyoxalase I gene. (a) Chromosomes of *S. cerevisae* and *L. donovani* separated and visualized with ethidium bromide before blotting; (b) the same blot probed with *L. donovani* glyoxalase I gene probe for *L. donovani*. Arrow shows the hybridizing band of *L. donovani*. (C) Expression analysis of glyoxalase I gene in *L. donovani*. Northern blot analysis of mRNA from *L. donovani* promastigotes (log phase culture). Lane 1; molecular weight markers, lanes 2 and 3; total RNA from *L. donovani* AG83 and *L. donovani* 2001, respectively, probed with a 426 bp full-length glyoxalase I gene.

Northern blotting of total *L. donovani* RNA and PCR-generated 426-bp gene probe revealed a single transcript of ~3.8 kb (Fig. 3C). The presence of a single RNA band in the corresponding Northern blot analysis indicated further the existence of a single encoding gene.

Over-expression and purification of full-length L. donovani GLOI enzyme in E. coli

In order to characterize the recombinant protein, the encoding *L. donovani* GLOI sequence was cloned inframe in pET-30a expression vector with its own start ATG codon. The resultant pET-30a-*L. donovani* GLOI construct was transformed into *E. coli* and protein overexpression induced as described under Materials and methods. A protein with a molecular weight that matched the estimated ~24 kDa according to amino acid composition of *L. donovani* GLOI with His_6 tag and S-tag present at its N-terminal end was induced (Fig. 4A). The recombinant protein was purified on Ni^{2+}–NTA affinity chromatography column (Fig. 4B). Purification of His-tagged *L. donovani* GLOI by metal affinity chromatography yielded ~5 mg of pure protein from a 1-L bacterial culture.

In order to determine the number of subunits in the recombinant glyoxalase I, the homogeneous protein was cross-linked with the bifunctional reagent glutaraldehyde (0.1%, 0.05%, and 0.025% respectively) prior to electrophoresis on a 10% polyacrylamide gel in the presence of SDS (Fig. 4C). Lane 1 shows recombinant GLOI without glutaraldehyde showing a band size of ~23.44 kDa. The results in lane 2, 3, and 4 show recombinant GLOI cross-linked with 0.1%, 0.05%, and 0.025% of glutaraldehyde, respectively. Bands corresponding to GLOI dimer of ~46 kDa can be seen (Fig. 4C). Lysozyme (14.4 kDa) from chicken egg white, a known monomer when cross-linked with the bifunctional reagent glutaraldehyde on electrophoresis on a 10% polyacrylamide gel in the presence of SDS appeared as a band of ~14 kDa (data not shown).

Recombinant GLOI was used to raise polyclonal antibody in BALB/c mice as described under Materials and methods. The antiserum recognized ~24 kDa fusion protein on Western blot of purified recombinant *L. donovani* GLO-I fusion protein (Fig. 5A). A Western blot using size-fractionated parasite protein, the antiserum could detect a band of anticipated *L. donovani* GLOI size ~16 kDa in promastigote extracts, which is in agreement with the value calculated from the predicted sequence (Fig. 5B). A Western blot using promastigote (50 μg) and amastigote extracts (50 μg) did not show any detectable difference with the polyclonal antiserum (Fig. 5B). Expression of LdGLOI protein in promastigotes from AG83 strains varies during growth in culture (Figs. 5C, D, and E). Protein accumulation increased somewhat on a per cell basis from 24 h of growth (early log phase) to reach a maximum at 96 h (a late log phase) after which a slight decrease was observed as the cells reached stationary phase (120 h).

Leishmania donovani glyoxalase I activity

The kinetic parameters of recombinant *L. donovani* glyoxalase I were determined with trypanothione hemithioacetal as substrate. The effect of both the substrates namely reduced trypanothione (at fixed concentration of methylglyoxal) and methylglyoxal (at fixed concentration of reduced trypanothione) on glyoxalase I activity was studied using nickel as a cofactor. Increase in the concentration of either reduced trypanothione or methyglyoxal showed similar K_m values towards trypanothione hemithioacetal

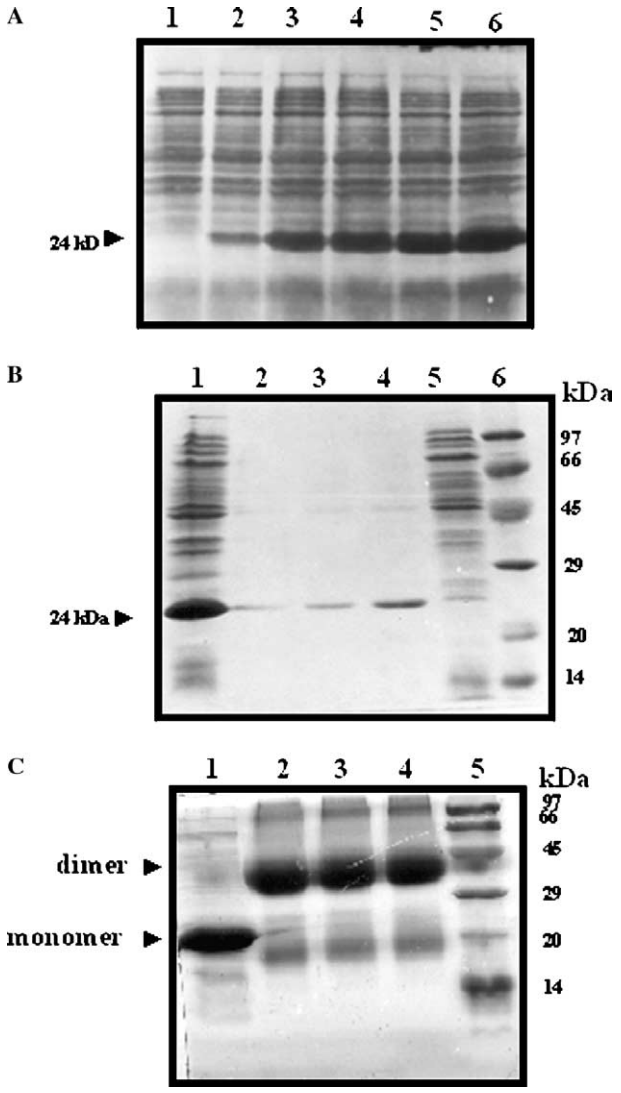

Fig. 4. Overexpression and purification of *L. donovani* glyoxalase I protein. (A) Coomassie blue staining of SDS–PAGE showing overexpression of full-length *L. donovani* glyoxalase I protein in *E. coli*. The pET-30a bacterial extract before induction (lane 1) and after induction (lanes 2–6) at 15, 30 min, 1, 2, and 3 h, respectively with 0. 5 mM IPTG. Arrow shows the induced recombinant glyoxalase I protein. Broad range protein MW marker (Bio-Rad) was used to identify the size of the recombinant protein. (B) Purification of glyoxalase I protein on Ni^{2+} affinity resin. Lane 1, induced crude lysate; lanes 2–4, eluted fractions showing purified glyoxalase I protein from the affinity column; lane 5, supernatant from the crude lysate; lane 6, broad range protein MW marker (Bio-Rad). (C) Analysis of subunit structure of glyoxalase I protein. Protein samples were run on a 10% SDS–polyacrylamide gel. Lane 1, glyoxalase I without cross-linkage treatment; lanes 2, 3, and 4 glyoxalase I cross-linked with 0.1%, 0.05%, and 0.025% gluteraldehyde respectively; lane 5, broad range protein MW marker (Bio-Rad).

as substrate (K_m 28.4 ± 3 μM). The *L. donovani* glyoxalase I showed a marked preference for trypanothione hemithioacetal as substrate over glutathione hemithioacetal (data not shown). Recombinant *L. donovani* glyoxalase I had specific activity of 340×10^4 nmol min^{-1} mg^{-1} protein and that of the native enzyme from the crude Leishmania lysate was 340 nmol min^{-1} mg^{-1} protein using trypanothione hemithioacetal as substrate.

Overexpression of glyoxalase I in L. donovani

To evaluate the consequences of GLOI overexpression, GLOI protein was measured in wild type and GLOI overexpressors. Western blot analysis of wild and GLOI overexpressing cell extract demonstrated a marked increase in GLOI protein in the overexpressors (Fig 6A). Northern blot analysis of wild and GLOI overexpressing cells showed overexpression of GLOI transcript (Fig. 6B).

Glyoxalase I inhibitor profiles

The IC_{50} values of known inhibitors of human and yeast glyoxalase I were obtained for both the wild type and overexpressing *L. donovani* strains (Table 1). There was no difference in the IC_{50} values between the wild type and overexpressing strains with hydroxynaphthoquinone derivative lapachol ($IC_{50} \sim 94$ μM) and quercetin ($IC_{50} \sim 26$ μM). Purpurogallin, another known inhibitor of human and yeast glyoxalase I, has an IC_{50} of 70 μM for the wild type and 132 μM for the GLOI overexpressing *L. donovani.* Flavones have been reported to be potential inhibitors of glyoxalase I [35]. In the present study, the IC_{50} value of flavone was found to be ~56 μM for the wild type *L. donovani* strain and ~70 μM for the GLOI overexpressing *L. donovani*. Glyoxalase I overproducer exhibited significant resistance to purpurogallin and flavone. In contrast, the IC_{50} values of wild type and GLOI overproducer for lapachol and quercetin were equivalent (Table 1).

3-D model of L. donovani glyoxalase I

The sequence of LdGLOI could be fitted comfortably onto the fold of *E. coli* GLOI with all the regular secondary structure elements conserved. The regions of alignment between the template and the model sequences involving insertions/deletions of residues have been modeled using the database searching mentioned under Materials and methods. The energy minimization resulted in stereochemically sound model with no short contacts between non-bonded atoms. Fig. 7 shows the superposition of the Cα traces of the model and the template structure with some of the functionally important residues shown.

Several crystal structures of human GLOI are available bound to ligands which give an opportunity to understand the structural basis of substrate specificity. It is known that both *E. coli* and human homologues of GLOI form dimers. Ligand bound complex structure of human GLOI (Fig. 8) shows that the two subunits interact closely with residues from both the subunits participating in the ligand recognition. The available structural knowledge about such ligand binding is extrapolated to the structural model of LdGLOI in order to understand the different substrate specificity of LdGLOI compared to *E. coli* GLOI.

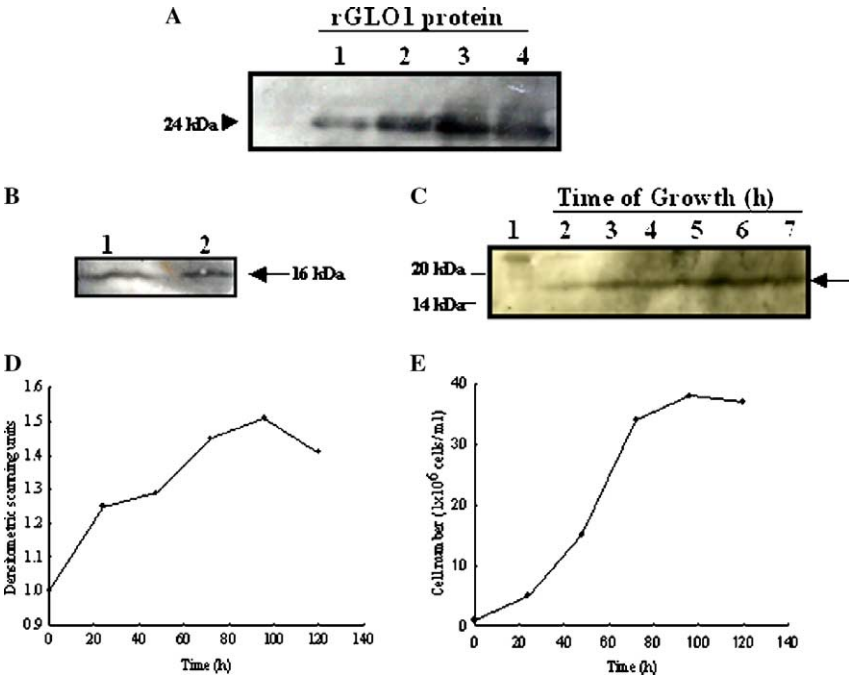

Fig. 5. Western blotting using anti-His-GLOI antibody. (A) Western blot analysis of different concentrations of purified GLOI-His fusion recombinant protein (lanes 1–4 containing 0.15, 0.30, 1.5, and 3.0 μg of recombinant protein, respectively). Prestained broad range protein molecular weight marker (Bio-Rad) was used to identify the size of the recombinant protein on the Western blot. (B) Western blot analysis of cell extracts of promastigotes (lane 1) and amastigotes (lane 2) reacted with anti-His-GLOI antibody. Arrow shows the position of the *L. donovani* GLOI. (C) Abundance of GLOI protein during the growth of *L. donovani* promastigotes. Promastigotes of strain AG83 were harvested at different times during growth in culture and proteins were separated by SDS–PAGE. Western blot shows 0.1 μg of purified His-GLOI fusion protein (lane 1); a leishmanial promastigote cell extract (50 μg per lane) at 0 h (lane 2); 24 h (lane 3); 48 h (lane 4); 72 h (lane 5); 96 h (lane 6); and 120 h (lane 7). (D) Densitometric scanning of the Western blot in (C). The bands were quantified by scanning on a densitometer and signal intensities relative to the zero point control are plotted. (E) Growth of wild type *L. donovani*. Parasites were enumerated every 24 h by counting in a hemocytometer. All these experiments were repeated thrice with essentially similar results.

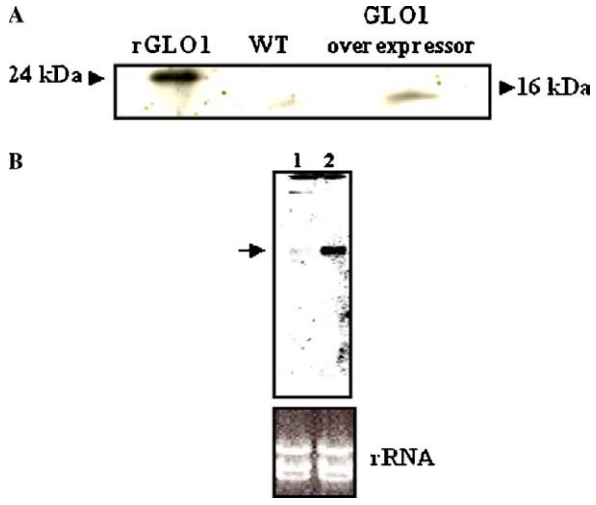

Fig. 6. Analysis of (A) protein and (B) RNA from wild type *L. donovani* (WT) and GLOI overexpressor. Recombinant GLOI protein (rGLOI) (1 μg) was used as a control. Polyclonal antiserum against *L. donovani* GLOI generated in mice was used to detect GLOI protein in fractionated extracts obtained from cultures harvested after 48 h of growth. (B) Total RNA was isolated from log phase culture of *L. donovani* wild type promastigotes (lane 1) and GLOI overexpressor (lane 2). Total RNA was electrophoresed, transferred to a membrane, and probed with a 426 bp full-length GLOI gene as described under Materials and methods. Ethidium bromide stained RNA gel showing equal loading of the RNA is shown. The results shown are from a single experiment typical of at least three giving identical results.

Table 1
Effect of over expression of glyoxalase I on the cytotoxicity of glyoxalase I inhibitors

Inhibitors	IC_{50} values (μM)	
	WT	GLOI overexpressor
Purpurogallin	70 ± 10	132 ± 4
Flavone	56 ± 2.6	69 ± 5.3
Quercetin	26 ± 1.8	27 ± 3.5
Lapachol	93 ± 3.5	96 ± 5.3

IC_{50} represents the concentrations of the drugs, which inhibited the growth of wild type and overexpressors by 50%. Each value is a mean of three independent experiments.

Discussion

All organisms require systems to shield them from chemical stress, such as the antioxidant enzymes that detoxify endogenous oxidants and the enzymes that metabolize exogenous toxins. However, endogenous toxins such as the reactive α-oxoaldehyde, methylglyoxal, are also byproducts of metabolism [6]. Methylglyoxal reacts rapidly with both proteins and nucleic acids and thus is both toxic and mutagenic [5,36]. Methylglyoxal is formed mainly by the degradation of triose phosphates, and also

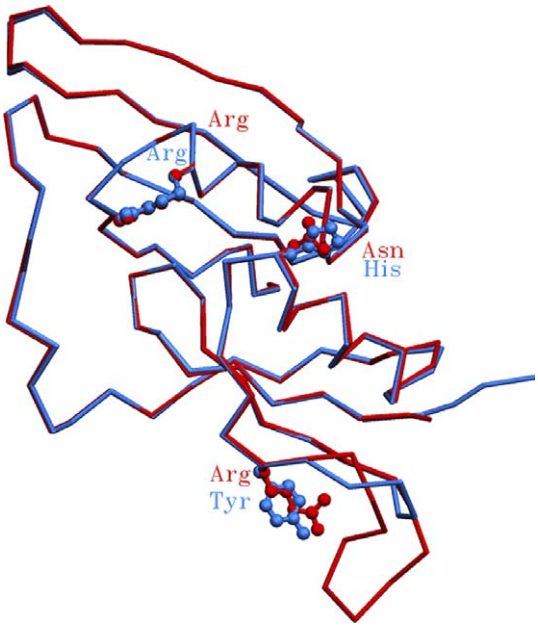

Fig. 7. Superposition of Cα traces of the crystal structure of *E. coli* GLOI (red) [20] and the model of LdGLOI (blue). Clear difference in the size and shape of the substrate-binding loop (near Arg to Tyr substitution) can be seen. Side chains of two of the critical residues (Arg and Tyr in LdGLOI) and another residue proximal to the functional site (His in LdGLOI) are also shown. This figure has been prepared using Setor software [45]. (For interpretation of the references to colour in this figure legend, the reader is referred to the web version of this paper.)

by metabolism of ketone bodies, threonine degradation, and the fragmentation of glycated proteins [37,38]. The glyoxalase system is a ubiquitous detoxification pathway that protects against cellular damage caused by methylglyoxal. Glyoxalase I (EC 4.4.1.5) is part of the glyoxalase system present in the cytosol and it prevents the accumulation of these reactive α-oxoaldehydes and thereby suppresses α-oxoaldehyde-mediated glycation reactions [7]. It is a key enzyme of the anti-glycation defence. Glyoxalase I converts the hemithioacetal, which is formed spontaneously from methylglyoxal and glutathione, into *S*-lactoylglutathione. The thioester is subsequently hydrolyzed by glyoxalase II yielding D-lactate and regenerating glutathione. In kinetoplastid organisms trypanothione replaces glutathione in the glyoxalase system [16,39]. Characterization of recombinant *L. major* glyoxalase I showed it to be unique among eukaryotic enzymes since it uses trypanothione hemithioacetal as the substrate instead of glutathione hemithioacetal [16]. In *Trypanosom brucei* glyoxalase II strongly prefers thioesters of trypanothione instead of glutathione as substrate [39].

To date, glyoxalase I sequences have been reported in several species including prokaryotes, plants, mammals, and yeast [40–42]. The human, bacterial and plant glyoxalase I are dimeric. The yeast enzymes of *S. cerevisae* and *Saccharomyces pombe* are monomers of 32 and 37 kDa, respectively. The sequence identity of human glyoxalase I

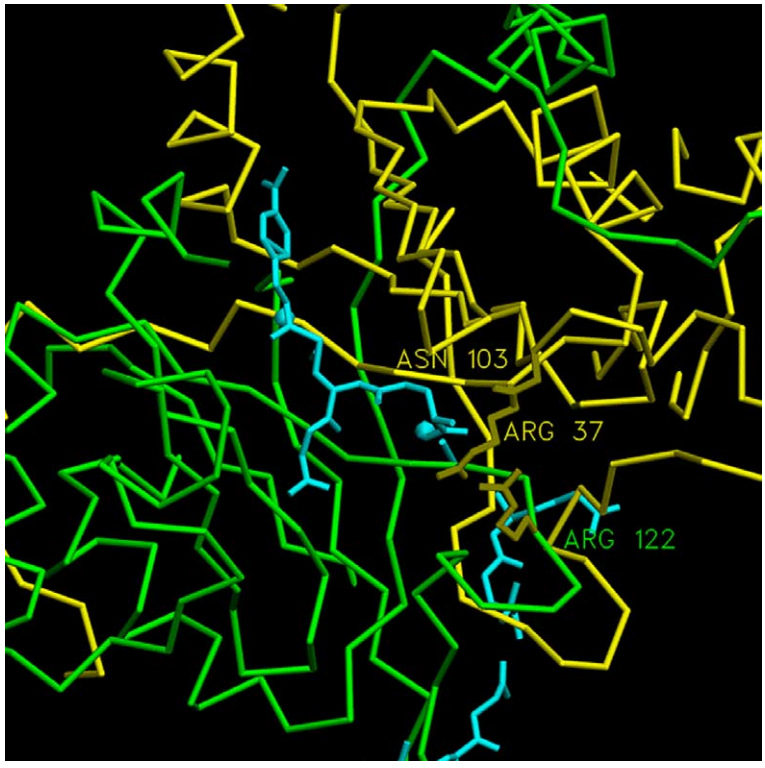

Fig. 8. Close-up of the substrate-binding site in the crystal structure of human GLOI bound to nitrobenzyloxycarbonylglutathione [19]. The C^{α} traces of the two closely interacting subunits of the dimeric human GLOI are shown in green and yellow. The transition-state analogue is shown in blue. The side chains of the three critical functional residues Arg 37 and Arg 103 (according to the residue numbering of human GLOI) from one of the two subunits and Arg 122 from the other subunit are shown. Arg 122 of the human GLOI corresponds to Tyr in LdGLOI. This figure has been prepared using Setor software [45]. (For interpretation of the references to colour in this figure legend, the reader is referred to the web version of this paper.)

with the bacterial enzyme (*Pseudomonas putida*) is 55% and with yeast enzyme between residues 1–182 and 183–326 (*S. cerevisiae*) is 47% suggesting that glyoxalase I of different origins may have arisen by divergent evolution from a common ancestor.

In this paper, we describe the molecular cloning and characterization of glyoxalase I from *L. donovani*, the most important pathogenic *Leishmania* species that is responsible for visceral leishmaniasis in India. The gene of glyoxalase I is located on chromosome 35. Comparison of the glyoxalase I from *L. donovani* and those of *L. major*, *L. infantum*, and *T. cruzi* protein showed 70% identity to *T. cruzi* lactoylglutathione lyase-like protein, 97% identity with *L. major* glyoxalase I, and 98% identity with *L. infantum* glyoxalase I protein. As in the case of *L. major* glyoxalase I the enzyme is trypanothione-dependent rather than glutathione-dependent. We have successfully cloned glyoxalase II (GLOII) from *L. donovani* (GenBank Accession No. AY851655) and there is only 30% identity between human GLOII and *L. donovani* GLOII sequence. Glyoxalase II recombinant fusion protein has a molecular mass of ~38 kDa and is a monomer. Glyoxalase II strongly prefers thioesters of trypanothione, instead of glutathione, as substrate (data not shown). Further characterization of glyoxalase II is presently going on in the laboratory.

Phylogenetic tree analysis showed a close evolutionary relationship of *L. donovani* and *T. cruzi* among the kinetoplastid protozoa. The kintoplastid GLOI sequences are closer to *E. coli* and *Synechococcus* sp. enzymes in phylogenetic analysis but no similarity with human, *M. musculus*, and *P. putida*.

Western blot analysis of whole cell lysates of promastigote of *L. donovani* using the polyclonal antibody against GLOI enzyme shows a single band of approximately 16-kDa and the same antibody recognized the recombinant protein of about 24 kDa expected size of the GLOI-His tag fusion protein. Cross-linking studies established that the recombinant GLOI is a dimer of equal subunits. Expression of LdGLOI protein in promastigotes from AG83 strains varies during growth in culture. Maximum protein accumulation was observed at 96 h (a late log phase). Sequence analysis of *L. donovani* glyoxalase I protein for metal binding showed high degree of conservation of the metal-binding residue between the trypanosomatid and *E. coli* GLOI enzymes. Recombinant parasite glyoxalase I enzyme required nickel for its activity thereby further confirming its close relationship to *E. coli* glyoxalase I enzyme. Earlier studies have shown that recombinant *L. major* glyoxalase I is unique among eukaryotic enzymes since it uses nickel as a cofactor, a property seen in *E. coli* enzyme [16]. *L. donovani* GLOI showed high level of specificity for trypanothione hemithioacetal and little activity with glutathione-hemithioacetal.

Previous studies have shown enhanced levels of glyoxalase I protein in human tumor tissues when compared to corresponding normal tissues [43]. In an attempt to study the significance of this overexpression, we transfected the *L. donovani* with glyoxalase I gene. Overexpression of glyoxalase I in transfectants was observed both by Northern and Western blot analysis. Inhibitors of glyoxalase I are known to be potential anticancer and antimalarial agents [43,12]. In this report, we evaluated, effect of several of the compounds that have been previously reported to have adverse effect on the human and yeast glyoxalase I enzyme, on both wild type and overexpressing *L. donovani* cells [44]. The IC_{50} values of several known inhibitors of human and yeast glyoxalase I showed that the compounds tested were weak inhibitors of *L. donovani* growth (lapachol, $IC_{50} = 100\ \mu M$ and quercetin IC_{50} of 26 μM in *L. donovani* compared to 0.35–0.7 μM for lapachol and IC_{50} of 10 μM for quercetin in human). Weak response of *L. donovani* to known inhibitors of glyoxalase I is a highly significant observation and could be related to the structural differences between the parasite and the host enzyme. When the cells were treated with purpurogallin or flavone, known inhibitor of human and yeast glyoxalase I, the transfectant cell line exhibited approximately 1.8- and 1.2-fold resistance, respectively, to the cytotoxic effects of these inhibitors when compared to control cell lines. However, hydroxynapthoquinone derivatives lapachol and quercetin did not show any difference in the IC_{50} values between the control and overexpressing cells.

While there are a number of important residues involved in the ligand binding to human GLOI, there are three critical residues essential for the function and these residues are also proximal to the substrate. Following the residue numbering of LdGLOI, the residues in the human homologue, Arg 8 and Asn 63 from a subunit in the dimer and Arg 101 in the other subunit, are the critical residues involved in function and also in ligand binding. These residues correspond to positions 37, 103, and 122, respectively, according to the numbering followed in the crystal structure of human GLOI complexed to a transition state analogue, Nitrobenzyloxycarbonylglutathione [19]. A close-up of the structure of Nitrobenzyloxycarbonylglutathione bound to the human GLOI is shown in Fig. 8. Out of the three crucial residues Arg 8 and Asn 63 (following the numbering of LdGLOI) are absolutely conserved in the members of the family (Fig. 1). Interestingly, Arg 101 is conserved or conservatively substituted by Lys in all homologues except in those from *Leishmania* organisms. In the homologues from *Leishmania* organisms, this Arg residue is replaced by Tyr. Remarkably, Tyr in this position is also present in the GLOI of *T. cruzi*. Thus, it appears that presence of Tyr in this alignment position is possibly a property of those homologues which are known to be or expected to be specific to trypanothione. Presence of very different residues, Arg (positively charged) and Tyr (aromatic, uncharged polar), present, respectively, in glutathione-specific and trypanothione-specific GLOI can be expected to play a crucial role indictating the specificity apart from other key changes as discussed below.

The critical Tyr 101 of LdGLOI model is located in a region of insertions/deletions (Fig. 1) corresponding to the substrate-binding loop. Considering this loop region there are two key distinguishing features between glutathione and trypanothione-specific homologues. First, as also noted by Vickers et al. [16], the number of residues in various glutathione-specific enzymes is more than that in the substrate-binding loop of trypanothione-specific homologues (Fig. 1). This results in a substantially long and bulky loop in the case of glutathione-specific enzymes compared to trypanothione-specific homologues. This change in the loop size also results in entirely different conformations and overall shapes of these loops. Fig. 7 shows the superposition of the crystal structure of *E. coli* GLOI and the modeled structure of LdGLOI. The clear changes in size and shape of the substrate-binding loop can be appreciated.

Second, as can be seen in Fig. 1, the substrate-binding loop of glutathione-specific GLOI sequences such as homologues from human and *E. coli* contains a substantial number of positively charged residues apart from a few acidic residues. However in the case of trypanothione-specific GLOI sequences such as those from *L. donovani* and *T. cruzi*, the substrate-binding loop is generally devoid of positively charged amino acids. This difference can also possibly influence the substrate-specificity.

Finally, in view of the uniqueness of *L. donovani* glyoxalase I enzyme, it could be exploited for structure-based drug designing of selective inhibitors against the parasite. Further work related to gene-knockout of glyoxalase I is presently going on to elucidate the importance of this enzyme in *L. donovani*.

Acknowledgments

A Senior Research Fellowship from the Council of Scientific and Industrial Research, India, supported A.M. K.P. is supported by a grant from the University Grants Commission, New Delhi, India. Sushma Singh thanks the Council of Scientific and Industrial Research for the award of a Junior Research Fellowship. We thank the project worker Mayurbhai H. Sahani, who participated in some experiments presented here. N.S. is an International Senior Fellow of the Wellcome Trust, London. He also thanks the Department of Biotechnology, New Delhi, for support in the form of computational genomics project.

References

[1] P. Aggarwal, R. Handa, S. Singh, J.P. Wali, Kala-azar: New development in diagnosis and treatment, Indian J. Pediatr. 66 (1999) 63–71.

[2] J.D. Berman, Treatment of New World cutaneous and mucosal leishmaniasis, Clin. Dermatol. 14 (1996) 519–522.

[3] E.A. Khalil, A.M. Hassan, E.E. Zijlstra, F.A. Hashim, M.E. Ibrahim, H.W. Ghalib, M.S. Ali, Treatment of visceral leishmaniasis with sodium stibogluconate in Sudan: management of those who do not respond, Ann. Trop. Med. Parasitol. 92 (1998) 151–158.

[4] V. Amato, J. Amato, A. Nicodemo, D. Uip, V. Amato-Neto, M. Durate, Treatment of mucocutaneous leishmaniasis with pentamidine isethionate, Ann. Dermatol. Venérelo. 125 (1998) 492–495.

[5] W.C.T. Lo, M.E. Westwood, A.C. McLellan, T. Selwood, P.J. Thornalley, Binding and modification of proteins by methylglyoxal under physiological conditions: a kinetic and mechanistic study with *N* alpha-acetylarginine, *N* alpha-acetylcysteine, and *N* alpha-acetyllysine, and bovine serum albumin, J. Biol. Chem. 269 (1994) 32299–32305.

[6] P.J. Thornalley, Pharmacology of methylglyoxal: formation, modification of proteins and nucleic acids, and enzymatic detoxification—a role in pathogenesis and antiproliferative chemotherapy, Gen. Pharmacol. 27 (1996) 565–573.

[7] S.J. Carrington, K.T. Douglas, The glyoxalase enigma—the biological consequences of a ubiquitous enzyme, IRCS Med. Sci. 14 (1986) 763–768.

[8] A.C. McLellan, P.J. Thornalley, Glyoxalase activity in human red blood cells fractioned by age, Mech. Ageing Dev. 48 (1989) 63–71.

[9] M.L. Clapper, S.J. Hoffman, K.D. Tew, Glutathione *S*-transferases in normal and malignant human colon tissue, Biochem. Biophys. Acta 1096 (1991) 209–216.

[10] F.M. Ayoub, R.E. Allen, P.J. Thornalley, Inhibition of proliferation of human leukaemia 60 cells by methylglyoxal in vitro, Leuk. Res. 17 (1993) 397–401.

[11] L.G. Egyud, A. Szent-Gyorgyi, Cancerostatic action of methylglyoxal, Science 160 (1968) 1140.

[12] P.J. Thornalley, M. Strath, R.J. Wilson, Antimalarial activity in vitro of the glyoxalase I inhibitor diester, *S*-p-bromobenzylglutathione diethyl ester, Biochem. Pharmacol. 47 (1994) 418–420.

[13] C. D'Silva, S. Daunes, P. Rock, V. Yardley, S.L. Croft, Structure–activity study on the in vitro antiprotozoal activity of glutathione derivatives, J. Med. Chem. 43 (2000) 2072–2078.

[14] N.D. Thomas, J.J. Blum, D-Lactate production by *Leishmania braziliensis* through the glyoxalase pathway, Mol. Biochem. Parasitol. 28 (1988) 121–128.

[15] K. Ghoshal, A.B. Banerjee, S. Ray, Methylglyoxal-catabolizing enzymes of *Leishmania donovani* promastigotes, Mol. Biochem. Parasitol. 35 (1989) 21–29.

[16] T.J. Vickers, N. Greig, A.H. Fairlamb, A trypanothione-dependent glyoxalase I with a prokaryotic ancestry in *Leishmania major*, Proc. Natl. Acad. Sci. USA 101 (2004) 13186–13191.

[17] A.C. Aronsson, E. Marmstal, B. Mannervik, Glyoxalase I, a zinc metalloenzyme of mammals and yeast, Biochem. Biophys. Res. Commun. 81 (1978) 1235–1240.

[18] S.L. Clugston, J.F. Barnard, R. Kinach, D. Miedema, R. Ruman, E. Daub, J.F. Honek, Overproduction and characterization of a dimeric non-zinc glyoxalase I from *Escherichia coli*: evidence for optimal activation by nickel ions, Biochemistry 37 (1998) 8754–8763.

[19] A.D. Cameron, M. Ridderstrom, B. Olin, M.J. Kavarana, D.J. Creighton, B. Mannervik, Reaction mechanism of glyoxalase I explored by an X-ray crystallographic analysis of the human enzyme in complex with a transition state analogue, Biochemistry 38 (1999) 13480–13490.

[20] M.M. He, S.L. Clugston, J.F. Honek, B.W. Matthews, Determination of the structure of *Escherichia coli* glyoxalase I suggests a structural basis for differential metal activation, Biochemistry 39 (2000) 8719–8727.

[21] P.S. Doyle, J.C. Engel, P.F. Pimenta, P.P. da Silva, D.M. Dwyer, *Leishmania donovani*: long-term culture of axenic amastigotes at 37 °C, Exp. Parasitol. 73 (1991) 326–334.

[22] V. Bellofato, G.A. Cross, Expression of a bacterial gene in a trypanosomatid protozoan, Science 244 (1989) 1167–1169.

[23] S.F. Altschul, T.L. Madden, A.A. Schaffer, J. Zhang, Z. Zhang, W. Miller, D.J. Lipman, Gapped BLAST and PSI-BLAST: a new generation of protein database search programs, Nucleic Acids Res. 25 (1997) 3389–3402.

[24] C.D. Lu, A.T. Abdelal, The gdhB gene of *Psuedomonas aeruginosa* encodes an arginine-inducible NAD(+)-dependent glutamate

dehydrogenase which is subject to allosteric regulation, J. Bacteriol. 183 (2001) 490–499.
[25] M.M. Bradford, A rapid and sensitive method for the quantitation of microgram quantities of protein utilizing the principle of protein-dye binding, Anal. Biochem. 72 (1976) 248–254.
[26] E. Racker, The mechanism of action of glyoxalase, J. Biol. Chem. 190 (1951) 685–696.
[27] D.L. Vander Jagt, L.P. Han, C.H. Lehman, Kinetic evaluation of substrate specificity in the glyoxalase-I-catalyzed disproportionation of—ketoaldehydes, Biochemistry 11 (1972) 3735–3740.
[28] D.L. Vander Jagt, E. Daub, J.A. Krohn, L.P. Han, Effects of pH and thiols on the kinetics of yeast glyoxalase I: an evaluation of the random pathway mechanism, Biochemistry 14 (1975) 3669–3675.
[29] B. Papadopoulou, G. Roy, M. Ouellette, A novel antifolate resistance gene on the amplified H circle of *Leishmania*, EMBO J. 11 (1992) 3601–3608.
[30] N. Srinivasan, T.L. Blundell, An evaluation of the performance of an automated procedure for comparative modelling of protein tertiary structure, Protein Eng. 6 (1993) 385–392.
[31] T.L. Blundell, D. Carney, S. Gardner, F. Hayes, B. Howlin, T. Hubbard, J. Overington, D.A. Singh, B.L. Sibanda, M. Sutcliffe, 18th Sir Hans Krebs lecture. Knowledge-based protein modelling and design, Eur. J. Biochem. 172 (1988) 513–520.
[32] C.M. Topham, A. McLeod, F. Eisenmenger, J.P. Overington, M.S. Jhonson, T.L. Blundell, Fragment ranking in modelling of protein structure. Conformationally constrained environmental amino acid substitution tables, J. Mol. Biol. 229 (1993) 194–200.
[33] M.J. Sutcliffe, F.R. Hayes, T.L. Blundell, Knowledge based modelling of homologous proteins, Part II: Rules for the conformations of substituted side chains, Protein Eng. 1 (1987) 385–392.
[34] S.J. Weiner, P.A. Kollman, D.A. Case, U.C. Singh, C. Ghio, G. Alagona, S. Profeta, P. Weiner, A new force field for molecular mechanical simulation of nucleic acids and proteins, J. Am. Chem. Soc. 106 (1984) 765–784.
[35] R.E. Allen, T.W. Lo, P.J. Thornalley, Inhibitors of glyoxalase 1 design, synthesis, inhibitory characteristics and biological evaluation, Biochem. Soc. Trans. 21 (1993) 535–540.
[36] U.M. Marinari, M. Ferro, L. Sciaba, R. Finollo, A.M. Bassi, G. Brambilla, DNA-damaging activity of biotic and xenobiotic aldehydes in Chinese hamster ovary cells, Cell Biochem. Funct. 2 (1984) 243–248.
[37] P.J. Thornalley, The glyoxalase system in health and disease, Mol. Aspects Med. 14 (1993) 287–371.
[38] P.J. Thornalley, Glutathione-dependent detoxification of alpha-oxoaldehydes by the glyoxalase system: involvement in disease mechanisms and antiproliferative activity of glyoxalase I inhibitors, Chem. Biol. Interact. 111–112 (1998) 137–151.
[39] T. Irsch, R.L. Krauth-Siegel, Glyoxalase II of African trypanosomes is trypanothione-dependent, J. Biol. Chem. 279 (2004) 22209–22217.
[40] A. Kimura, Y. Inoue, Glyoxalase I in micro-organisms: molecular characteristics genetics, and biochemical regulation, Biochem. Soc. Trans. 21 (1993) 518–521.
[41] R. Deswal, T.N. Chakaravarty, S.K. Sopory, The glyoxalase system in higher plants: regulation in growth and differentiation, Biochem. Soc. Trans. 21 (1993) 527–530.
[42] E. Marmstal, A.C. Aronsson, B. Mannervik, Comparison of glyoxalase I purified from yeast (*Saccharomyces cerevisiae*) with the enzyme from mammalian sources, Biochem. J. 183 (1979) 23–30.
[43] D.J. Creighton, Z.B. Zheng, R. Holewinski, D.S. Hamilton, J.L. Eiseman, Glyoxalase I inhibitors in cancer chemotherapy, Biochem. Soc. Trans. 31 (2003) 1378–1382.
[44] K.T. Douglas, D.I. Gohel, I.N. Nadvi, J. Quilter, A.P. Seddon, Partial transition state inhibitors of glyoxalase I from human erythrocytes, yeast and rat liver, Biochem. Biophys. Acta 829 (1985) 109–118.
[45] S.V. Evans, SETOR: Hardware lighted three-demensional solid model representations of macromolecules, J. Mol. Graphics 11 (1993) 134–138.